JOURNAL OF THERMOPHYSICS AND HEAT TRANSFER
Vol. 11, No. 3, July–September 1997

# Transient Radiation Transport in Participating Media Within a Rectangular Enclosure

Kunal Mitra,* Ming-Sing Lai,† and Sunil Kumar‡
*Polytechnic University, Brooklyn, New York 11201*

**This paper outlines the formulation of the two-dimensional transient radiation transport through a scattering–absorbing medium. The $P_1$ approximation in a Cartesian coordinate system is invoked to simplify the transient radiative transfer equation because it is very complicated to solve in its general form. A boundary-driven radiative problem is considered in which the radiation intensities at some areas on a surface are modeled as boundary conditions and maintained at constant values in all angular directions.**

## Nomenclature

$c$ = speed of light in the medium
$D$ = nondimensional optical thickness
$g$ = integrated phase function
$H$ = Heaviside unit step function
$I$ = scattered radiation intensity
$I_B$ = directionally uniform boundary intensity
$L$ = width over which boundary source is present
$P_n$ = Legendre polynomial
$p$ = scattering phase function
$Q_x$ = nondimensional radiative flux in $X$ direction
$Q_y$ = nondimensional radiative flux in $Y$ direction
$q_x$ = radiative flux in $x$ direction
$q_y$ = radiative flux in $y$ direction
$S$ = source term
$T$ = nondimensional time
$t$ = time
$U$ = nondimensional intensity averaged over all directions
$u$ = intensity averaged over all directions
$W$ = nondimensional optical lateral width of the medium
$X, Y$ = nondimensional space coordinate
$x, y$ = Cartesian space coordinate
$\theta$ = polar angle measured from the positive $x$ axis
$\mu$ = cos $\theta$
$\sigma_a$ = absorption coefficient
$\sigma_e$ = extinction coefficient, $\sigma_a + \sigma_s$
$\sigma_s$ = scattering coefficient
$\phi$ = azimuthal angle
$\Omega$ = solid angle
$\omega$ = scattering albedo

## I. Introduction

MOST previous studies of radiative transfer through scattering–absorbing medium assume the radiation transport to be steady state. Benchmark numerical results for the steady-state problem are available for semi-infinite and thick mediums.[1,2] The steady-state radiative transfer problem for a gray absorbing and emitting medium in a rectangular enclosure is considered using the $P_N$ approximation.[3] A steady-state two-dimensional analysis that computes the transfer of solar or thermal radiation through cloudy atmospheres with arbitrary optical properties has been reported in the literature.[4] A survey of radiation heat transfer steady-state mathematical formulation in multidimensional scattering–absorbing media geometries is also available from the literature.[5,6] However, a two-dimensional transient problem that needs attention and has not been considered in the literature is the backscattering or transmission of a laser beam by a multiple scattering medium when the incident laser beam is normal to the surface of the media.

With the advent of short pulse lasers and their rapid deployment in a variety of engineering applications such as ocean and atmosphere remote sensing,[7] optical tomography,[8] laser surgery,[9] and combustion product characterization and combustion diagnostics,[10] the traditional steady-state radiative transfer formulations cannot be used to analyze their interaction with participating media. A one-dimensional transient solution for radiative transfer for one-dimensional geometry for the case of laser incidence on the surface and propagating at speed $c$ inside the scattering–absorbing medium has been developed and reported in the literature.[11] It is shown that the results obtained by the consideration of the complete hyperbolic transient radiative transfer equations are significantly different than the commonly used equations obtained by neglecting the transient terms or by considering the transport via a transient diffusion formulation. This difference is pronounced during the initial transients and therefore is important for analyzing short time data. The work[11] is extended in the present study to two-dimensional Cartesian geometries. In this paper the first step in analyzing the transient radiative transfer in a two-dimensional Cartesian coordinate system has been taken for the case of a boundary-driven problem in which the driving radiation intensity is maintained at a constant magnitude on parts of the bounding surface. The $P_1$ approximation is used to analyze the two-dimensional effects in a scattering–absorbing media having a rectangular geometry.

Even though steady-state studies[5,10] have shown that the $P_1$ approximation for the intensity distribution is not as accurate as more sophisticated approximations and that the $P_1$ approximation fails to match the correct propagation speed,[11] the $P_1$ method is used in the study because of the following considerations. The present study is the first attempt at solving the transient two-dimensional case, and the more sophisticated approximations have been found to be mathematically and numerically intractable at this juncture. Convergence is very difficult to obtain for higher-order approximations that would exhibit better accuracy and signal propagation speeds. In con-

Received Sept. 19, 1996; revision received Jan. 13, 1997; accepted for publication Jan. 14, 1997. 

*Research Associate, Department of Mechanical Engineering, 6 Metrotech Center; currently at National Oceanic and Atmospheric Administration, Environmental Research Laboratories, 325 Broadway, Boulder, CO 80303.

†Graduate Research Assistant, Department of Mechanical Engineering, 6 Metrotech Center.

‡Associate Professor, Department of Mechanical Engineering, 6 Metrotech Center. Associate Member AIAA.

trast, the $P_1$ method is computationally efficient and convergence is always obtained. Also, the trends obtained by varying different parameters are expected to exhibit the same characteristics as the other methods, albeit with less accuracy. Since the present study seeks to examine the unique characteristics and unique qualitative trends and variations of the transmission results of the two-dimensional wave-like transient radiative transfer equation, the $P_1$ approximation is therefore appropriate and is thus utilized.

In this study the transient radiative transfer equation in two-dimensional geometry is solved numerically for the first time. The effects of boundary source width, lateral width, properties, and different boundary conditions on the transmission results are analyzed. The boundary-driven problem is considered to highlight the results, such as transmitted flux, during the initial transients. Comparisons with the diffusion approximation and with the steady-state values at long times are also made. The boundary source is turned on at an initial time and maintained for all times, except for one case where the boundary source is applied for a certain time and then shut off.

## II. Theory

The physical case under consideration is a two-dimensional scattering and absorbing medium in a Cartesian coordinate system in which radiation is maintained at the surface at a constant value in all directions. The geometry of the problem considered is a $x$-$y$ coordinate system being infinite in the $z$ direction (see Fig. 1). The radiative transfer equation assuming constant properties can be written as[12–14]

$$\frac{1}{c}\frac{\partial I(x, y, \theta, \phi, t)}{\partial t} + \cos\theta\frac{\partial I(x, y, \theta, \phi, t)}{\partial x} + \sin\theta\cos\phi\frac{\partial I(x, y, \theta, \phi, t)}{\partial y} = -\sigma_e I(x, y, \theta, \phi, t) + \frac{\sigma_s}{4\pi}\int_{4\pi} I(x, y, \theta', \phi', t)p(\theta', \phi' \rightarrow \theta, \phi)\,\mathrm{d}\Omega' + S(x, y, \theta, \phi, t) \tag{1}$$

The term $\cos\theta$ represents the direction cosine in the positive $x$ direction and $\sin\theta\cos\phi$ is the direction cosine with respect to the positive $y$ axis (see Fig. 1). Equation (1) is an integro-differential equation where the partial differentials correspond to a hyperbolic differential equation that yields wave solutions.

The scattering phase function can be represented as a series of $P_n$ by the following[14,15]:

$$p(\theta, \phi \rightarrow \theta', \phi') = \sum_{n=0}^{N} a_n P_n(\cos\theta)P_n(\cos\theta') + 2\sum_{n=1}^{N}\sum_{m=1}^{n} a_n\frac{(n-m)!}{(n+m)!}P_m^n(\cos\theta)P_m^n(\cos\theta')\cos n(\phi - \phi') \tag{2}$$

where $N$ is the order of anisotropy of the scattering phase function, and $a_n$ are the coefficients in the expansion and $a_0 = 1$.

The $P_1$ approximation is used to analyze the transient radiative transfer equation in the two-dimensional geometry. For the boundary-driven problem, $S$ vanishes from Eq. (1) and the source of radiation is introduced through one of the boundaries of the medium. Since the objective of the study is to seek simple leading-order solutions that give insight to the behavior of the radiation transport through the media, the radiative transfer equation is integrated and solutions that satisfy the integrated equation are evaluated. Integrating Eq. (1) with respect to the solid angle $\mathrm{d}\Omega$ and repeating the integration after multiplying Eq. (1) with $\cos\theta$ and $\sin\theta\cos\phi$ yields a set of

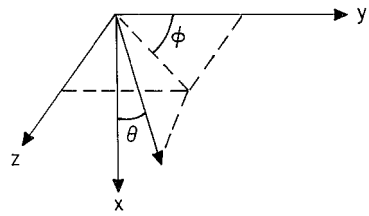


**Fig. 1 Schematic of the coordinate system.**

equations that can be simplified by introducing the linear approximation intensity distribution[11]:

$$I(x, y, \theta, \phi, t) = u(x, y, t) + \cos\theta(3/4\pi)q_x(x, y, t) + \sin\theta\cos\phi(3/4\pi)q_y(x, y, t) \tag{3}$$

where

$$u(x, y, t) = \frac{1}{4\pi}\int_{4\pi} I(x, y, \theta, \phi, t)\,\mathrm{d}\Omega \tag{4a}$$

$$q_x(x, y, t) = \int_{4\pi} I(x, y, \theta, \phi, t)\cos\theta\,\mathrm{d}\Omega \tag{4b}$$

$$q_y(x, y, t) = \int_{4\pi} I(x, y, \theta, \phi, t)\sin\theta\cos\phi\,\mathrm{d}\Omega \tag{4c}$$

The resultant equations can be expressed as the following:

$$\frac{4\pi}{c}\frac{\partial u(x, y, t)}{\partial t} + \frac{\partial q_x(x, y, t)}{\partial x} + \frac{\partial q_y(x, y, t)}{\partial y} + 4\pi\sigma_a u(x, y, t) = 0 \tag{5a}$$

$$\frac{1}{c}\frac{\partial q_x(x, y, t)}{\partial t} + \frac{4\pi}{3}\frac{\partial u(x, y, t)}{\partial x} + (\sigma_e - \sigma_s g)q_x(x, y, t) = 0 \tag{5b}$$

$$\frac{1}{c}\frac{\partial q_y(x, y, t)}{\partial t} + \frac{4\pi}{3}\frac{\partial u(x, y, t)}{\partial y} + (\sigma_e - \sigma_s g)q_y(x, y, t) = 0 \tag{5c}$$

where $g$ is given by

$$g = \frac{3}{4\pi}\frac{1}{4\pi}\int_{4\pi}\int_{4\pi} p(\Omega' \rightarrow \Omega)\cos\theta'\cos\theta\,\mathrm{d}\Omega'\,\mathrm{d}\Omega = \frac{3}{4\pi}\frac{1}{4\pi}\int_{4\pi}\int_{4\pi} p(\Omega' \rightarrow \Omega)\sin\theta'\cos\phi' \times \sin\theta\cos\phi\,\mathrm{d}\Omega'\,\mathrm{d}\Omega = \frac{a_1}{3} \tag{6}$$

The set of Eqs. (5a–5c) are nondimensionalized in the following manner:

$$X = x\sigma_e, \qquad Y = y\sigma_e, \qquad T = \frac{ct\sigma_e}{\sqrt{3}}$$
$$U = \frac{u}{I_B}, \qquad Q_x = \frac{q_x}{I_B}, \qquad Q_y = \frac{q_y}{I_B}, \qquad \omega = \frac{\sigma_s}{\sigma_e} \tag{7}$$

The nondimensional form of Eq. (5) becomes

$$\frac{\partial U}{\partial T} + \frac{\sqrt{3}}{4\pi}\frac{\partial Q_x}{\partial X} + \frac{\sqrt{3}}{4\pi}\frac{\partial Q_y}{\partial Y} + \sqrt{3}(1 - \omega)U = 0 \tag{8a}$$

$$\frac{\partial Q_x}{\partial T} + \frac{4\pi}{\sqrt{3}}\frac{\partial U}{\partial X} + \sqrt{3}(1 - \omega g)Q_x = 0 \tag{8b}$$

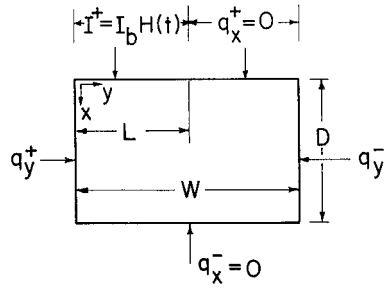


**Fig. 2 Schematic of the boundary conditions considered.**

$$\frac{\partial Q_y}{\partial T} + \frac{4\pi}{\sqrt{3}}\frac{\partial U}{\partial Y} + \sqrt{3}(1 - \omega g)Q_y = 0 \tag{8c}$$

The boundary conditions are such that the intensities pointing to the inside of the medium are zero, i.e., for the $P_1$ approximation (see Fig. 2)

$$\int_{2\pi} I \, d\Omega = 0 \tag{9}$$

where $2\pi$ represents the hemisphere pointing inward to the inside of the medium, except at the areas that provide the source of radiation. For this study only the driving boundary condition is at $X = 0$ surface, for which the boundary condition is given by the following expression:

$$I(X = 0,\ 0 \le Y \le L,\ \cos\theta > 0,\ \phi,\ T) = I_B H(T) \tag{10}$$

where $L$ is the nondimensional lateral width ($0 < L \le W$) and $H(T)$ is the Heaviside function. The nondimensional optical thicknesses of the medium are $W$ in the $Y$ direction and $D$ in the $X$ direction. The boundary conditions for other surfaces can be represented by the following equations:

$$Q_x^-(X = D,\ Y,\ T) = 0 \tag{11a}$$

$$Q_y(X,\ Y = 0,\ T) = 0 \tag{11b}$$

$$Q_y^-(X,\ Y = W,\ T) = 0 \tag{11c}$$

where the superscripts $+$ and $-$ represent the positive and negative coordinate axes, respectively.

The boundary conditions on the four boundaries for the previous system of equations as given by Eqs. (10) and (11) can be represented in terms of the variables $U$, $Q_x$, and $Q_y$ as

$$\begin{aligned} &U(X = 0,\ 0 \le Y \le L,\ T) \\ &\quad = (-1/2\pi)Q_x(X = 0,\ 0 \le Y \le L,\ T) + H(T) \\ &U(X = 0,\ L < Y \le W,\ T) \\ &\quad = (-1/2\pi)Q_x(X = 0,\ L < Y \le W,\ T) \end{aligned} \tag{12a}$$

$$U(X = D,\ Y,\ T) = (1/2\pi)Q_x(X = D,\ Y,\ T) \tag{12b}$$

$$Q_y(X,\ Y = 0,\ T) = 0 \tag{12c}$$

$$U(X,\ Y = W,\ T) = (1/2\pi)Q_y(X,\ Y = W,\ T) \tag{12d}$$

To verify the computational methodology and the computer programs, the two-dimensional results are compared with the one-dimensional results. This is done by replacing the boundary condition for the two-dimensional geometry given by Eqs. (11c) and (12d) by

$$Q_y(X,\ Y = W,\ T) = 0 \tag{12e}$$

and by considering the source to be over the entire surface, i.e., between 0 and $W$ at $X = 0$ surface. This represents the case for which the boundaries in the lateral direction are insulated. Other boundary conditions on the lateral surface are also used and they are indicated later in the text.

The set of equations given by Eq. (8) is solved by a half-node discretization technique.[16] By this method the $U$ values are computed at half-distances ahead of flux for the hyperbolic equations for satisfying the stability criteria. The intensities and fluxes at the boundaries are also discretized similar to that of the governing equation.

## III. Results and Discussions

The two-dimensional radiative transfer equation in a Cartesian coordinate system is solved using $P_1$ approximation for the case of the boundary-driven problem formulation. Different magnitudes of the area over which boundary sources are applied are considered, as are different boundary conditions on the lateral boundaries. The effects of property variations inside the medium are also analyzed. The transmission results obtained for various cases represent $Q_x^+$ at $X = D$ for varying locations in the $Y$ direction.

### A. Validation of Two-Dimensional Model

The validity of the results of the two-dimensional $P_1$ approximation is examined by comparison with the one-dimensional case. For this purpose, the two-dimensional boundary conditions for heat flux in the lateral direction $Q_y$ are kept zero (insulated boundaries) on both sides and the driving boundary conditions are applied over the entire width ($0 \le Y \le H = W$) at $X = 0$.

The one- and two-dimensional transmission results for $D = 1.0$, $\omega = 0.9$, $g = 0.215$, and $W = 1.0$ (for a two-dimensional case) are plotted in Fig. 3 for diffuse boundary radiation of constant magnitude in all directions. The one-dimensional results are obtained both by the method of characteristics and the finite difference half-node discretization technique. The two-dimensional results are obtained numerically using the half-node discretization technique. The one- and two-dimensional results overlap each other suggesting that the two-dimensional formulation is as accurate as the one-dimensional. The values of grid sizes ($\Delta X$ and $\Delta Y$) and temporal node size ($\Delta T$) are varied by one order in either direction and the results are found to be stable and converging. But there is a slight difference in the time when the first significant transmitted signal is observed, which is the time taken by the photons to traverse the depth of the medium, between grid sizes $\Delta X = \Delta Y = 10^{-2}$ and $\Delta X = \Delta Y = 10^{-3}$. The finer the grid sizes, the more accurate the results. By further reducing the grid sizes the numerical solution and the one-dimensional solution, obtained by the method of characteristics, match each other. Coarse grids cannot adequately represent the sharp wave front of the radiation signal and tend to smear the front, leading to photons being predicted to arrive faster than the signal speed predicted

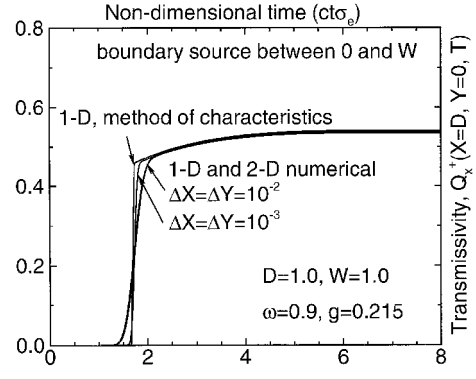


**Fig. 3 Comparison of one- and two-dimensional transmitted flux for establishing validity of numerical results.**

by the method of characteristics. The value of $\Delta X = \Delta Y = 10^{-2}$ is used from Figs. 4–11 because it is noticed from Fig. 3 that finer grid sizes improve the prediction of propagation speed, but the magnitude of the transmissivity is almost identical for both grid sizes.

Note that the wave speed for the $P_1$ method is $c/\sqrt{3}$ as discussed in the literature.[11] The wave front therefore arrives at time $ct\sigma_e = \sqrt{3}D$. Detailed discussions of the signal speed (or wave speed) of the $P_1$ method can be found elsewhere.[11]

### B. Effect of Boundary Source Width

The transmitted flux for the two-dimensional case is plotted in Figs. 4a and 4b for different boundary source widths. Here, $Q_y(Y = 0) = Q_y(Y = W) = 0$ and the medium under consideration has $D = 1.0$, $W = 1.0$, and $\omega = 0.9$. Transmitted flux at $X = D$ and at different $Y$ coordinate locations along the lateral direction are examined. It is seen that the transmitted flux decreases along an increasing coordinate location in the lateral direction because of the increase in the mean distance from the boundary source. The transmitted flux is zero initially until the optical signal from the nearest point of the source traverses the depth of the medium, it then reaches a maximum value after which it starts to decrease. The maximum value is reached when wave fronts from all points of the boundary source have reached the location at which the transmission is being measured. The reduction following the peak may be attributed to the outscattering from lines of sight between the source and detector. But the transmitted flux again increases because of the reflection of waves from the boundaries. Insulated boundary conditions imply that the thermal/radiative reflection of waves occur from the boundaries of the medium. The boundaries of the medium do not reflect or emit any radiation intensity. After long time periods, the flux reaches a constant steady-state value. The magnitude of the transmitted flux does not vary with the lateral location for a boundary source located over the entire width between 0 and $W$. But for other values of boundary source width, the transmission varies along the lateral direction and the highest magnitude is at $Y = 0$. The reflection phenomenon is not because of numerical oscillations as the results are thoroughly tested by using different grid sizes for temporal and spatial nodes and the consideration of different boundary source widths.

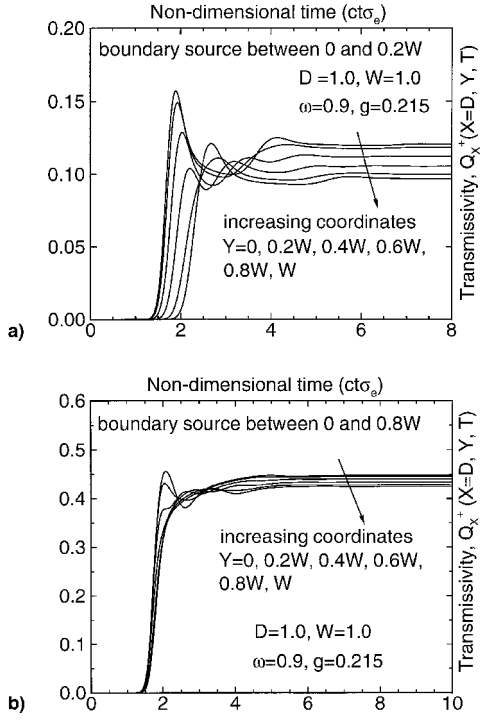


**Fig. 4 Transmitted flux for boundary source between a) 0–0.2$W$ and b) 0–0.8$W$.**

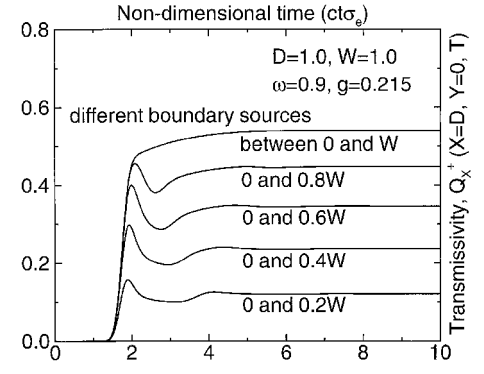


**Fig. 5 Comparison of the transmitted flux for different boundary source widths.**

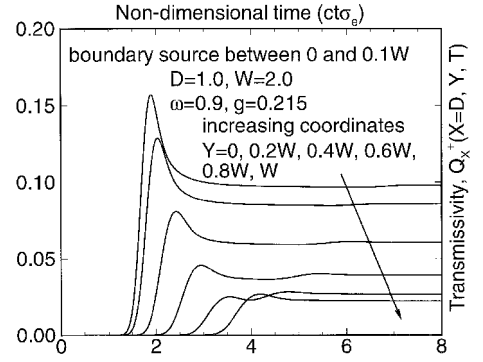


**Fig. 6 Transmitted flux for $D = 1.0$, $W = 2.0$, and $\omega = 0.9$ for a boundary source between 0–0.1$W$.**

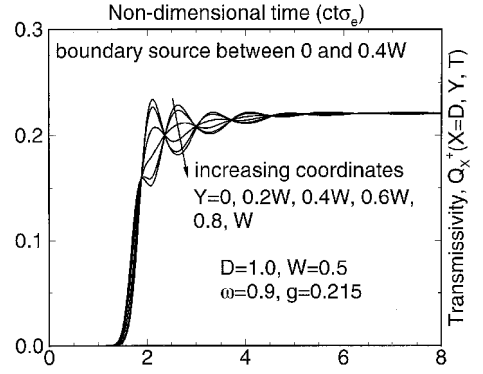


**Fig. 7 Transmitted flux for $D = 1.0$, $W = 0.5$, and $\omega = 0.9$ for a boundary source between 0–0.4$W$.**

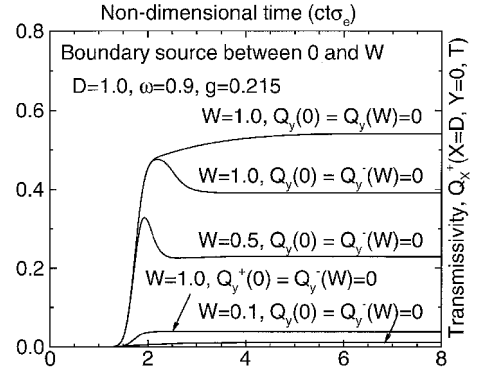


**Fig. 8 Comparison of the transmitted flux for different boundary conditions and varying $W$.**

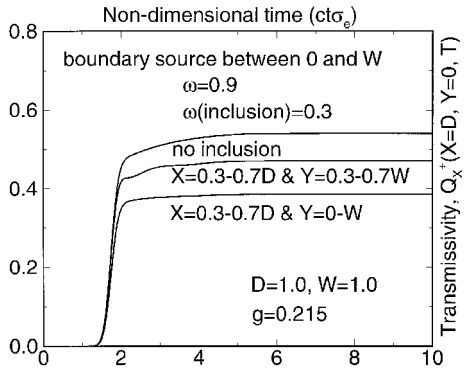


**Fig. 9 Comparison of the transmitted flux for varying properties inside the medium.**

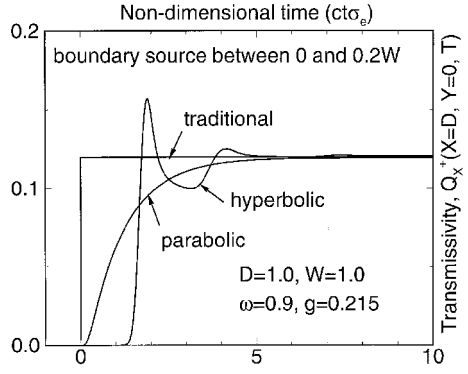


**Fig. 10 Comparison of the transmitted flux for hyperbolic, parabolic, and traditional $P_1$ models.**

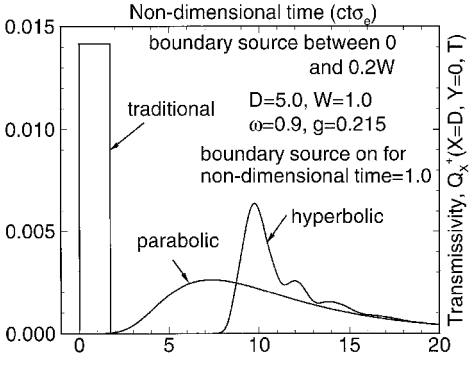


**Fig. 11 Comparison of the transmitted flux for hyperbolic, parabolic, and traditional $P_1$ models for the source pulsed in time.**

In Fig. 5 the transmitted flux at $Y = 0$ is shown for different boundary source widths for the same parameters and boundary conditions as in Fig. 4. The boundary condition of $Q_y(Y = W) = 0$ implies a boundary where the reflection of waves takes place. The greater the width of the boundary source, the higher the transmitted flux. The smaller the width of boundary sources, the longer the time period when the reflection of the transmitted signal at $Y = W$ occurs, because the radiation from the boundary source has to travel larger distances before being reflected.

### C. Effect of Lateral Width

Figures 6 and 7 show the two-dimensional transmitted flux for $W = 2.0$ and 0.5, respectively, and having $D = 1.0$ and $\omega = 0.9$. For these cases and that in Fig. 4a, the boundary conditions and the boundary source width (=0.2) are the same. The smaller the $W$, the larger the amount of multiple reflections of waves from the boundary before the transmitted value reaches a constant steady-state value will be. When the value of $W$ is large, the reflection of waves may not be felt because of the attenuation over the large distance. Hence, multiple peaks for the transmitted flux are observed in Fig. 7 because the lateral width is the least among different cases considered.

### D. Effect of Different Lateral Boundary Conditions

Three different boundary conditions are considered to study their effect on the transmission results for a source spanning the entire boundary, i.e., between 0 and $W$ at $X = 0$. These are a, $Q_y(Y = 0) = Q_y(Y = W) = 0$; b, $Q_y(Y = 0) = Q_y^-(Y = W) = 0$; and c, $Q_y^+(Y = 0) = Q_y^-(Y = W) = 0$. Case a represents the case where the boundary conditions in the lateral direction are insulated, and therefore loss of energy occurs only through the top and bottom surfaces. In case b there is loss of energy through the $Y = W$ boundary, whereas for case c, energy is lost from all four surfaces of the medium. The two-dimensional transmitted flux at $Y = 0$ is plotted as a function of time for different boundary conditions and lateral width dimensions as shown in Fig. 8. The magnitude of the transmitted flux for the case of boundary condition $Q_y(Y = W) = 0$ (case a) is independent of $W$ and behaves as a one-dimensional medium (cf., Fig. 3). But the transmitted flux for boundary condition $Q_y^-(Y = W) = 0$ (case b), which implies a nonreflecting boundary, is a strong function of lateral width. The transmitted flux for the boundary condition $Q_y^+(Y = 0) = 0$ and $Q_y^-(Y = W) = 0$ (case c) has the least magnitude because both of the boundaries are nonreflecting in nature. For case a, the transmitted flux has a higher magnitude because the energy is kept inside the medium because of the reflection of waves from the boundaries. For the case of $Q_y^-(Y = W) = 0$, the transmitted flux is also plotted as a function of the lateral width of the medium. For smaller lateral widths the value of the transmitted flux is smaller since the corresponding ratio of the surface area through which energy leaves to the scattering volume is increased. The same phenomena is magnified for the boundary condition $Q_y^+(Y = 0) = 0$ and $Q_y^-(Y = W) = 0$ because both lateral boundaries lose energy.

### E. Effect of Properties

Figure 9 shows the effects of property variations inside the medium when both lateral boundaries are insulated (case a). If $\omega$ is 0.9 throughout the medium, higher values of transmission are obtained as compared to media in which lower albedo (more absorbing) inclusions are present. For an inclusion having a partial albedo of 0.3 within the medium of albedo of 0.9, there is not only a decrease in the magnitude of the transmitted flux, but an inflection is observed in the temporal signal of the transmitted flux distribution. The inflection is prominent for the case where the inclusion is at the center of the medium, but is not observed when the inclusion spans the entire width. This is because the presence of the lateral boundaries of the inclusion inside the medium introduce the inflection. The occurrence of this inflection is significant because it can provide information about the presence of some inhomogeneity inside the medium. The internal boundaries of the inhomogeneity inside the medium are treated as nonreflecting.

### F. Comparison Between Different Simplifications of the $P_1$ Model

The transmissivity at $Y = 0$ for hyperbolic, parabolic, and traditional $P_1$ models for a boundary source between $0–0.2W$ is plotted in Fig. 10. The parabolic solution is determined by dropping the time derivative term from Eqs. (8b) and (8c), whereas the traditional method solution is obtained by dropping the time derivative term from Eqs. (8a–8c). Since there is no explicit time derivative in the traditional method, any time variation is introduced through the driving boundary conditions only. The hyperbolic model attains multiple peaks because of the reflection from the boundaries of the medium, whereas the parabolic model attains a steady-state value without undergoing any such reflections at the boundaries. The

parabolic model predicts a transmission value even at small times, indicating a physically unrealistic propagation speed that is greater than the speed of light. The hyperbolic model does not suffer from such drawbacks. The transmissivity for the traditional case remains at a constant value because the source remains on at all times and the results follow the time variation of the source. The constant value of the transmission shown by the traditional method will therefore remain as long as the source stays on. This implies an infinite speed of propagation since transmission is observed at the same instant that the source is turned on. Both the hyperbolic and parabolic models reach the same steady-state values after long times.

For all cases considered previously the boundary source is present at all times. To examine the difference in the predicted transmission signals when the source is shut off, the nondimensional transmissivity at $Y = 0$ is plotted for hyperbolic, parabolic, and traditional methods in Fig. 11 for the case in which the source is shut off after a finite time (i.e., the source is pulsed in time). As indicated previously, the temporal variation of the transmission mimics that of the source for the traditional method. The transmissivity predicted by the traditional method thus drops to zero as soon the source is shut off. It must be noted that the source is on for a nondimensional time of unity as defined by Eq. (7). Therefore this corresponds to $ct\sigma_e = \sqrt{3}$. The hyperbolic and parabolic models predict finite values of transmission for time periods after the source is shut off. This corresponds to the finite time taken by the photons to escape from the medium after multiple scattering within the medium.

## IV. Conclusions

The present study is the first one to examine the modeling of transient radiative transfer in a two-dimensional enclosure using the complete hyperbolic formulation. The two-dimensional transmission results using the $P_1$ approximation are obtained for a variety of boundary conditions and medium dimensions. There is a significant difference in the transmission results depending upon the hyperbolic, parabolic, or traditional formulations selected. The effect of the presence of internal boundaries and/or refraction at the boundary of the medium can also be incorporated into the solution easily. The analysis of the nature of the transmission distribution is very important in different technologies. For example, it has tremendous potential in optical tomography to detect the presence of inhomogeneities such as tumors inside living tissues and organs. The study demonstrates that the complete radiative transfer equation yields significantly different results than the previously used diffusion and other models from the literature. An experimental study[17] has shown that the previous models fail to match experimental data. The present study is the first step toward more realistic two-dimensional modeling and the results of this model in the one-dimensional geometry[11] have been shown to qualitatively match experimental data better than the previous models. Future research is needed to extend the present formulations to cylindrical two- or three-dimensional geometries for which experimental data exist.

## Acknowledgment

The authors acknowledge the thoughtful comments by the reviewers whose suggestions improved the manuscript.

## References

[1]Crosbie, A. L., and Dougherty, R. L., "Two-Dimensional Linearly Anisotropic Scattering in a Semi-Infinite Cylindrical Medium Exposed to a Laser Beam," *Journal of Quantitative Spectroscopy and Radiative Transfer*, Vol. 28, No. 3, 1982, pp. 233–263.

[2]Crosbie, A. L., and Dougherty, R. L., "Two-Dimensional Isotropic Scattering in a Finite Thick Cylindrical Medium Exposed to a Laser Beam," *Journal of Quantitative Spectroscopy and Radiative Transfer*, Vol. 27, No. 2, 1982, pp. 149–183.

[3]Ratzel, A. C., III, and Howell, J. R., "Two-Dimensional Radiation in Absorbing-Emitting Media Using $P_N$ Approximation," *Journal of Heat Transfer*, Vol. 105, 1983, pp. 333–340.

[4]Evans, K. F., "Two-Dimensional Radiative Transfer in Cloudy Atmospheres: The Spherical Harmonics Spatial Grid Method," *Journal of the Atmospheric Sciences*, Vol. 50, No. 18, 1993, pp. 3111–3124.

[5]Viskanta, R., "Radiation Heat Transfer: Interaction with Conduction and Convection and Approximate Methods in Radiation," *Proceedings of 7th International Heat Transfer Conference* (Munich, Germany), Vol. 1, 1982, pp. 103–121.

[6]Tan, Z., "Radiative Heat Transfer in Multidimensional Emitting, Absorbing, and Anisotropic Scattering Media—Mathematical Formulation and Numerical Method," *Journal of Heat Transfer*, Vol. 111, 1989, pp. 141–146.

[7]Weinman, J. A., and Shipley, S. T., "Effects of Multiple Scattering on Laser Pulses Transmitted Through Clouds," *Journal of Geophysical Research*, Vol. 77, 1972, pp. 7123–7128.

[8]Yamada, Y., "Light-Tissue Interaction and Optical Imaging in Biomedicine," *Annual Review of Fluid Mechanics and Heat Transfer*, edited by C. L. Tien, Vol. 6, Begell House, New York, 1995, pp. 1–59.

[9]Gemert, M. J. C., and Welch, A. J., "Clinical Use of Laser-Tissue Interaction," *IEEE Engineering in Medicine and Biology*, Dec. 1989, pp. 10–13.

[10]Mengüc, M. P., and Viskanta, R., "Comparison of Radiative Transfer Approximations for Highly Forward Scattering Planar Medium," *Journal of Quantitative Spectroscopy and Radiative Transfer*, Vol. 29, 1983, pp. 381–394.

[11]Kumar, S., Mitra, K., and Yamada, Y., "Hyperbolic Damped-Wave Models for Transient Light-Pulse Propagation in Scattering Medium," *Applied Optics*, Vol. 31, No. 19, 1996, pp. 3372–3378.

[12]Brewster, M. Q., *Thermal Radiative Transfer and Properties*, Wiley-Interscience, New York, 1992.

[13]Siegel, R., and Howell, J. R., *Thermal Radiation Heat Transfer*, 3rd ed., Hemisphere, Washington, DC, 1992.

[14]Modest, M. F., *Radiative Heat Transfer*, McGraw–Hill, New York, 1993.

[15]Kumar, S., and Felske, J. D., "Radiative Transport in a Planar Media Exposed to Azimuthally Unsymmetric Incident Radiation," *Journal of Quantitative Spectroscopy and Radiative Transfer*, Vol. 35, 1986, pp. 187–212.

[16]Richtmyer, R. D., and Morton, K. W., *Difference Methods for Initial Value Problems*, 2nd ed., Interscience, New York, 1967.

[17]Yoo, K. M., Liu, F., and Alfano, R. R., "When Does the Diffusion Approximation Fail to Describe Photon Transport in Random Media," *Physical Review Letters*, Vol. 64, 1990, pp. 2647–2650.